Original Article

In vivo Confocal Microscopic Evaluation of Corneal Changes in Acute Endothelial Rejection

Golshan Latifi[1], Ramon Katoozpour[1], Reza Ghaffari[1], Parisa Abdi[1], Maryam Kasiri[1], Sahar Berijani[1]

[1]Cornea Department, Farabi Eye Hospital, Tehran University of Medical Sciences, Tehran, Iran

Abstract

Purpose: To evaluate the microstructural corneal changes during acute endothelial graft rejection and following treatment using *in vivo* confocal microscopy (IVCM).

Methods: Patients with a clinical diagnosis of severe acute endothelial graft rejection following penetrating keratoplasty were included in this study. IVCM was performed on the 1st day the patient presented with rejection signs and at the time of clinical resolution.

Results: Twenty-three patients were included in this study. Inflammatory cells appeared as dendritic cells (DCs) and less frequently, as non-DCs in basal epithelial and subbasal areas. Activated keratocytes (AKs) (type 1: large cells with visible cytoplasmic processes; type 2: elongated and spindle-shaped keratocytes) were visible in acute phase. Following resolution, type 1 AKs considerably reduced, but type 2 cells were more often persisted. Multiple types of keratic precipitates (KPs) were also visible in acute phase which resolved following resolution of rejection.

Conclusions: Acute graft rejection was associated with an increase in the number of DCs, activation of keratocytes, and aggregation of various types of KPs. Inflammatory process subsided in almost all cases, but the IVCM changes did not return to normal early after clinical resolution of rejection.

Keywords: Activated keratocytes, Graft rejection, *In vivo* confocal microscopy, Keratic precipitate

Address for correspondence: Golshan Latifi, Cornea Department, Farabi Eye Hospital, Qazvin Square, Tehran, Iran.
E-mail: golshanlatifi@yahoo.com
Submitted: 30-Nov-2020; **Revised:** 07-Mar-2021; **Accepted:** 10-Mar-2021; **Published:** 22-Oct-2021

Introduction

Corneal graft rejection is the most common cause of graft failure.[1] It is mainly a cell-mediated immune response which is controlled by the $CD4^+$ T cells. Epithelial, subepithelial, and endothelial rejections are not discrete entities. Therefore, graft rejection is a comprehensive inflammatory process that involves the entire cornea and even anterior chamber (AC).[2]

In vivo confocal microscopy (IVCM), a noninvasive, real-time imaging modality allows detection of the cellular or even subcellular changes of the cornea. There are a limited number of published reports on cellular changes of graft rejection by IVCM.[3-7]

Access this article online

Quick Response Code:

Website: www.jcurrophthalmol.org

DOI: 10.4103/joco.joco_211_20

The first report of corneal changes during graft rejection by IVCM was published in 1995 when Cohen *et al*.[3] performed corneal transplantation in vascularized and high-risk graft bed of rabbit eyes. In their study, IVCM demonstrated foci of small round hyperreflective infiltrating cells in the graft stroma, but due to the low resolution of the device they used for imaging, no more details of the inflammatory process were discernible.

Understanding the structural changes of the cornea and the inflammatory process of acute graft rejection at a cellular level could help successful treatment and also prevention of subsequent rejection episodes.[5-7] Confocal microscopy helps to understand different aspects of the immunological events

How to cite this article: Latifi G, Katoozpour R, Ghaffari R, Abdi P, Kasiri M, Berijani S. *In vivo* confocal microscopic evaluation of corneal changes in acute endothelial rejection. J Curr Ophthalmol 2021;33:291-7.

that could eventually lead to reversible or irreversible graft damage. In this study, the *in vivo* characteristics of cornea in acute phase of graft rejection and after the resolution of the episode are evaluated.

Methods

This interventional case series was a parallel study with a previously conducted randomized clinical trial to assess the effect of topical tacrolimus as an adjuvant therapy in acute graft rejection, registered in Iranian Registry of Clinical Trials (IRCT, www.irct.ir) with the registration ID: IRCT2014040617088N1.[8]

The protocol of the current study was in accordance with the tenets of the Declaration of Helsinki and received ethical approval from the Institutional Review Board of Farabi Eye Research Center (ID: REC-93218). Informed written consent was obtained from all patients.

Patients with a clinical diagnosis of acute severe endothelial rejection following penetrating keratoplasty (PKP) were included in the study. Diagnostic criteria for severe endothelial graft rejection were stromal edema associated with (1) aqueous cells or (2) keratic precipitates (KPs) and/or endothelial rejection line in a previously clear PKP graft.[9]

Medical treatment was started based on the previously mentioned protocol (patients were randomized into two groups, one receiving conventional topical and subconjunctival steroid, and the second receiving adjuvant topical tacrolimus in addition to conventional therapy). Patients were followed for resolution of the graft rejection. At baseline (the 1st day the patient presented to the clinic with the sign and symptoms of acute rejection) and at the resolution of rejection, patients underwent assessment of visual acuity, slit-lamp examination, and confocal microscopy. Resolution of rejection was defined as clinical disappearance of corneal edema, KP, AC reaction, and other inflammatory signs such as conjunctival injection. Data from the two groups were analyzed as a whole in this study.

Severity of graft edema and KPs was graded 0–4+ based on the number of quadrants involved. AC reaction was graded (grade 0: <1 cell, grade 0.5+: 1–5 cells, grade 1+: 6–15 cells, grade 2+: 16–25 cells, grade 3+: 26–50 cells, grade 4+: >50 cells) based on the Standardization of Uveitis Nomenclature grading scheme.[10] Central corneal thickness measurements were done using CASIA (anterior segment optical coherence tomography, CASIA2, Tomey GmbH, Germany).

In vivo confocal microscopy imaging

IVCM with Heidelberg Retina Tomogram II-Rostock Cornea Module (HRTII-RCM, Heidelberg Engineering GmbH, Heidelberg, Germany) was performed in all patients by one experienced confocal microscopy technician (M. K). This is a laser scanning confocal microscope using a 670-nm red laser. It has an immersion lens with a magnification of ×63. Each image represented a coronal section of 400 × 400 μm at a selectable corneal depth. The IVCM scanning was performed from the central cornea and also from the area with maximum edema or inflammatory signs. A side-mounted digital camera attached to HRTII-RCM was used to help determine the location of the cornea being scanned. The automated section scan mode was used. Only images from the area with maximum inflammatory signs (edema and/or KP) were selected. The patients in whom severe edema precluded clear IVCM imaging of deep stroma and endothelium were excluded. Images were captured sequentially through the thickness of the cornea including epithelium and subbasal area, anterior stroma, middle and posterior stroma, and endothelium, giving a total of 200–300 frames per cornea.

For confocal microscopy, an anesthetic eye drop was first applied topically. A disposable cover (Tomo-Cap, Heidelberg, Germany) was mounted over the lens after covering the lens with 2.0 mg/g Carbomer, (Visicotears®, Alcon, Fort Worth, Texas, United States). A few drops of gel were also used to lubricate the Tomo-Cap surface. The patients were then asked to rest their chin on a chinrest, and their forehead in the microscope support and to look straight ahead at the microscope's white light.

Confocal microscopic image analysis

All images were analyzed by one observer (G. L.) who was masked to the rejection status (active rejection vs. resolved rejection) of the patients. For analysis of pathologic findings, 5–7 images from each layer (epithelium and subbasal area, anterior stroma, middle and posterior stroma, and endothelium) were analyzed to avoid artifacts or accidental findings. Three images of epithelium and Bowman's layer with the best resolution were selected and analyzed for the presence of inflammatory cells. Inflammatory cells included dendritic cells (DCs) defined as bright structures with multiple cytoplasmic processes measuring 25–50 μm in size [Figure 1a] or non-DCs (nDCs) defined as round-to-oval, irregular hyperreflective cellular structures of 10–40 μm in diameter without any visible cytoplasmic processes [Figure 1b].[11]

Endothelial cell changes and different morphologies of KPs were also evaluated. They included soft, large KPs, and adopted from Lim *et al*.[12] who described eight different morphologic types of KPs in uveitis patients. Other types included nodular KPs defined as small (4–20 μm), hyperreflective, round-to-oval objects without projections, stellate KPs defined as a large aggregation (>40 μm) of hyperreflective elements with projections, dendriform KPs defined as small (<40 μm), hyperreflective elements with long processes, granular KPs defined as hyperreflective dots (<4 μm) along with tiny dendriform and dash like KPs forming a small, polymorphous pattern, and cruciform KPs defined as hyperreflective elements with more than 1 thick projection [Figure 2].

Statistical analysis

The statistical analysis of data was carried out using the SPSS software version 25 (IBM Inc., Chicago, IL, USA). Descriptive

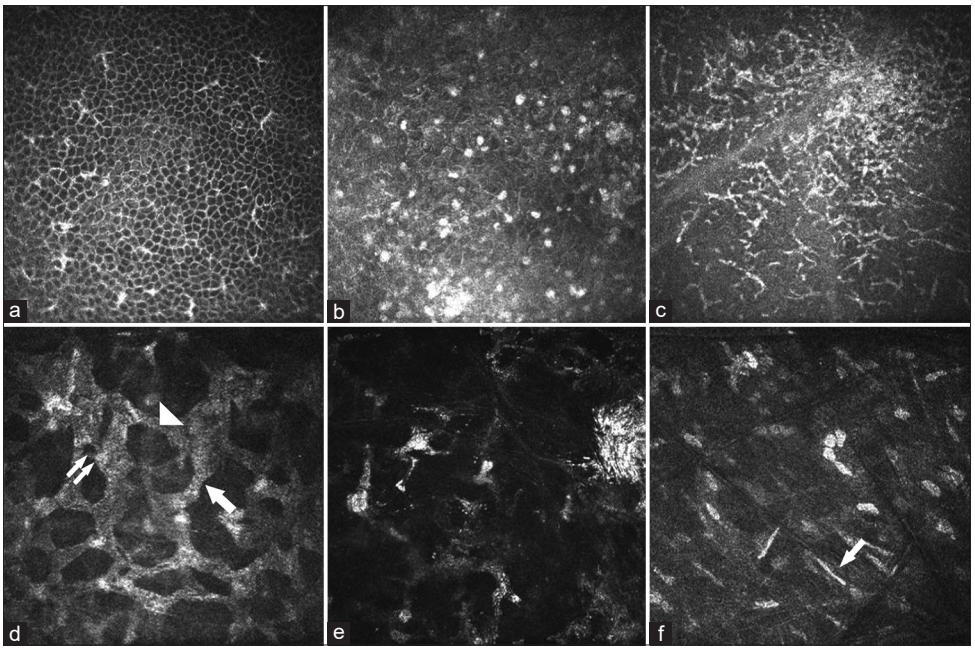

Figure 1: Inflammatory cells: Dendritic cells (DCs) defined as bright structures with multiple cytoplasmic processes measuring 25–50 μm in size in basal epithelial layer in a rejected graft (a), nondendritic cells defined as globular hyperreflective cellular structures without obvious cell processes measuring 10–40 μm in size in intermediate epithelial layer in a rejected graft (b), DCs forming a network with their interdigitating dendrites in acute rejection phase (c), active type 1 keratocytes with enlarged, prominent cytoplasm and cell processes (arrow), intercellular lacunes (arrowhead), intracellular vacuole (double arrows) (d), tiny hyperreflective dots visible in the cytoplasm of type 1 activated keratocytes in anterior stroma which could represent the intracellular activated organelles (e), active type 2 spindle-shaped keratocytes with elongated nucleus (arrow) (f)

statistics including mean, standard deviation, and range were used to show the distribution of the data. The Mann–Whitney U-test was used to compare the means.

Results

Twenty-three patients with acute graft rejection and adequate IVCM image quality (visible deep corneal layers) were included in this study. The mean age was 36.86 ± 18.20 years. Fifteen of these 23 patients had confocal images after resolution of rejection (7 patients did not have posttreatment confocal images, and 1 did not recover the graft rejection). Nine patients were treated with conventional topical and subconjunctival steroids, and 14 patients received topical tacrolimus 0.05% in addition to conventional therapy. Mean time from presentation (baseline) to resolution of grafts (time between 2 IVCM image acquisition) in 15 patients whose postresolution confocal images were available was 16.93 ± 10.35 (range, 7–40) days.

Table 1 shows demographic features and clinical signs at baseline.

Basal epithelial and subbasal inflammatory cells

Inflammatory cells appeared as either DCs [Figure 1a, 1c] or nDCs [Figure 1b].[11] These inflammatory cells were located between intermediate and basal epithelial cells and in subbasal area (Bowman's layer) where the subbasal nerve plexus resides.

Stromal and keratocyte changes

Two different morphological changes of keratocytes were visible. Type 1 activated keratocytes (AKs) [Figure 1d] defined as cells with enlarged, visible cytoplasm and interconnecting cell processes[13] [Figure 1d, arrow] were seen in 15 patients. Small dark round intracellular vacuoles near cell nuclei [Figure 1d, double arrow] and larger intercellular spaces named lacunes were visible between interconnected type 1 AKs [Figure 1d, arrow head]. As described before, tiny hyperreflective dots were visible in the cytoplasm of type 1 AKs in the anterior stroma of seven patients which could represent the intracellular activated organelles [Figure 1e].

Type 2 AKs seen in six patients were elongated spindle-shaped cells as hyperreflective short lines of various thicknesses in the stroma[13] [Figure 1f]. These cells were more numerous in anterior stroma which could represent active migratory keratocytes. In three patients whose confocal images were available after clinical resolution, these cells were still detectable.

After clinical resolution of graft rejection, AKs (large keratocytes with visible cell processes) were only detectable in two patients, in whom the activity of keratocytes (defined according to size and visibility of cell body and processes) decreased, but still, some morphological changes indicating activity were present [Figure 3c and d].

A pattern of stippled hyperreflective dots (<10 μ) confined to enlarged hyperreflective keratocytes of anterior stroma was detectable in seven patients [Figure 1e], which disappeared in 10 out of 15 patients, early after treatment.

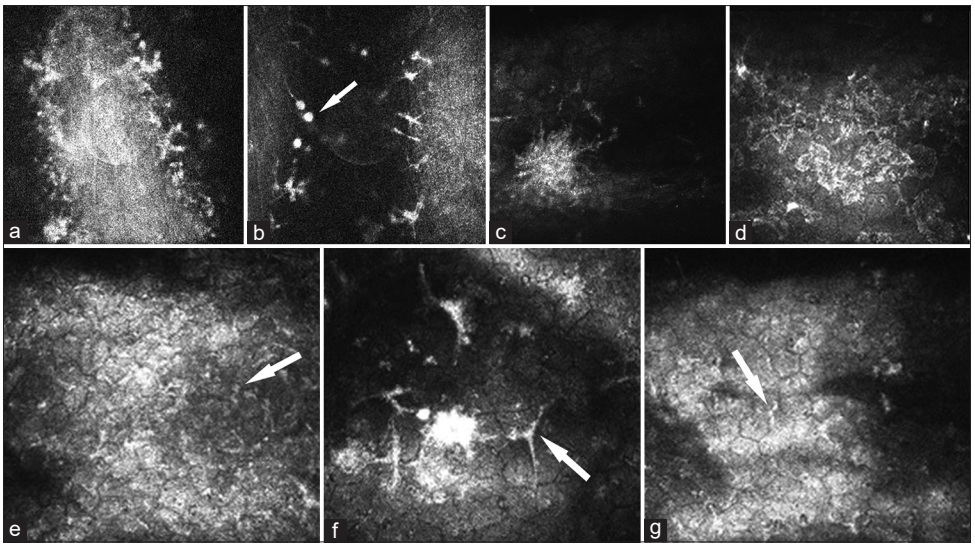

Figure 2: *In vivo* confocal microscopy images of the corneal endothelium in acute phase of rejection shows soft large keratic precipitate (KP) appearing as vary large (>100 μm) homogeneous object with medium reflectivity and numerous round to oval bright elements at its border (a), small (4-20 μm) hyperreflective round to oval object without projections as nodular KP (arrow) (b), large aggregation (>40 μm) of hyperreflective element with projections as stellate KP (c), crumb-like KP (d) hyperreflective dot (<4 μm) with small dendriform and dash like KPs forming a small polymorphous pattern as granular KP (arrow) (e), small (<40 μm) hyperreflective element with long processes as dendriform KP (arrow) (f), hyperreflective element with more than 1 thick projection as cruciform KP (arrow) (g)

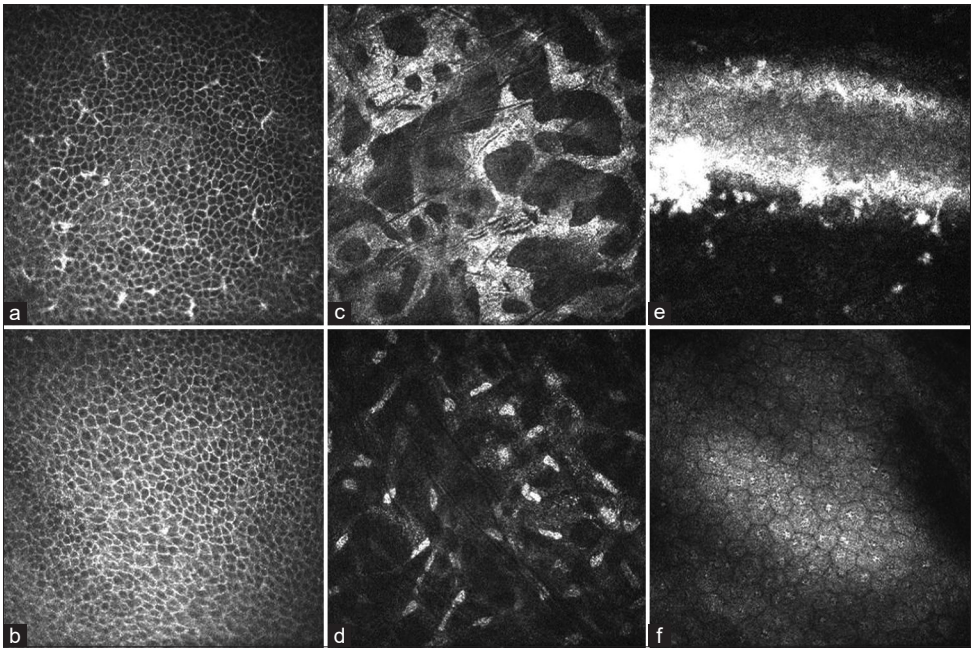

Figure 3: Representative images of different layers of the cornea at the time of graft rejection (a, c and e) and after resolution of rejection (b, d and f), basal epithelial layer: Multiple dendritic cells (a), almost no visible inflammatory cells (b), stroma: Visible enlarged cell processes of activated keratocytes (c), only nuclei of inactive keratocytes are visible (d), endothelium: Soft large keratic precipitate with no other discernible features of endothelial cells (e), hexagonal mosaic of endothelial cells with prominent cell nuclei (f)

Endothelial changes

Different types of KPs were observed in the acute phase of rejection. Most of the patients presented with three or more types of KPs at the same time. The most prevalent type was soft large KP [Figure 2a] which appeared as a very large (>100 μm) homogeneous object with medium reflectivity that usually was not confined to a single 400 × 400 μm confocal frame with numerous round-to-oval bright elements at its border. These large soft KPs were present in 14 patients. High reflectivity of these large KPs completely obscured the view of the endothelial cell. Nodular KPs were seen in 13 patients [Figure 2b], stellate KPs in 8 patients [Figure 2c], dendriform KPs in 7 patients [Figure 2g], granular KPs in 6 patients [Figure 2e], and cruciform KPs in 7 patients [Figure 2f]. A unique type of KP was observed in

one patient with a crumb-like appearance [Figure 2d] which completely resolved after resolution of rejection. This form of KP has not been described previously.

Details of endothelial cells were not visible in nine patients due to hyperreflectivity of KPs masking the background cells. Other detectable endothelial changes were pseudoguttae, dark spaces between endothelial cells [Figure 4a], polymorphism, polymegathism, and prominent endothelial cell nuclei appearing as round hyperreflective elements with irregular hyporeflectivity inside each endothelial cell [Figure 4b].

Following treatment, KPs completely disappeared in almost all patients, and only two of them still had a few detectable nodular KPs. The only remaining endothelial change after resolution of rejection was prominent endothelial nuclei which was detectable in 9 out of 15 available posttreatment confocal images. However, size and reflectivity of cell nuclei decreased following treatment [Figure 3e and f]. Table 2 summarizes the prevalence of main confocal features before and after treatment.

Table 1: Demographic features and clinical signs of the patients at baseline

Parameters	Values
Gender (male/female) (*n*)	16/7
Age (years)	36.86±18.20
BCVA at baseline (logMAR)	0.85±0.36
Pachymetry at baseline (μm), mean±SD	725.85±163.58
Duration of graft (months), mean±SD (range)*	19.85±10.79 (4.5-36)
Duration of acute rejection symptoms (days), mean±SD (range)**	7.48±5.06 (1-21)
Indications for graft, *n* (%)	
PBK	1 (4.3)
KCN	9 (39.1)
Corneal dystrophy	2 (8.7)
Corneal scar	10 (43.5)
Fungal keratitis	1 (4.3)
Clinical signs	
Edema, *n* (%)	
0+	0
1+	2 (8.7)
2+	6 (26.1)
3+	6 (26.1)
4+	9 (39.1)
KP, *n* (%)	
0+	1 (4.3)
1+	4 (17.4)
2+	8 (34.8)
3+	7 (30.4)
4+	3 (13)
AC reaction, *n* (%)†	0+
0+	4 (17.4)
1+	4 (17.4)
2+	1 (4.3)
3+	1 (4.3)
4+	1 (4.3)
Rejection line (*n*)	5/18

*Interval postgraft, **Time from appearance of patient-reported symptoms to visiting the clinic (baseline time), †Anterior chamber was not visible in 12 (52.2%) of patients. BCVA: Best corrected visual acuity, SD: Standard deviation, KP: Keratic precipitate, AC: Anterior chamber, PBK: Pseudophakic bullous keratopathy, KCN: Keratoconus

Discussion

In this study, inflammatory process of acute graft rejection was evaluated by IVCM. Moderate infiltration of DCs in subbasal area associated with underlying AKs, and appearance of numerous KPs, was seen in the process of graft rejection. Early after clinical resolution of rejection, the infiltration of activated DCs subsided and activity of keratocytes decreased; however, it did not return to normal [Figure 3].

Several studies have reported the location of DCs to be at the level of basal epithelium or between the nerve fibers beneath the basal epithelial cells in 35–60 μm depth.[11] They are primarily distributed at the corneal limbus and peripheral cornea and are occasionally visible at the central cornea in healthy eyes.[14] The density of DCs in noninflamed healthy grafts has a significant association with the risk of rejection. Higher leukocyte density in corneas without any sign of rejection indicated a subclinical inflammatory cellular response which was associated with a higher risk of rejection.[15] Subepithelial infiltrations in acute graft rejection were also shown to be focal accumulations of hyperreflective DCs at the level of the basal epithelium and Bowman's membrane.[4] Zhivov *et al*. showed that in healthy cornea, DCs could be found in only 31.3% of cases.[16] DCs, as antigen presenting cells, play an important role in the immunologic cascade of graft rejection. Mature DCs are defined by the increased number and length of cell processes on IVCM.[11,14,17] We observed an increased number of DCs with long processes representing an active mature phenotype in the central cornea at the time of acute rejection. Likewise, Chirapapaisan *et al*. showed a significant increase in corneal inflammatory cells, in the subbasal and endothelial layers in rejected grafts.[5] In clear grafts, only 16.7% have few activated DCs.[18]

The nDCs seen in confocal images, leukocytes infiltrating the cornea and participating in the immune response of rejection, are most probably T helper cells.

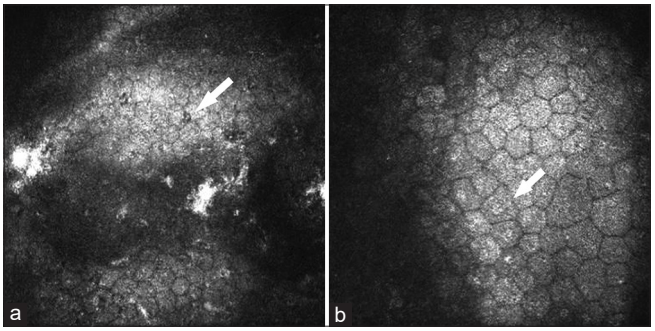

Figure 4: Dark spaces between endothelial cells and hyperreflective round objects inside each endothelial cell known as pseudoguttae (arrow) (a), visible endothelial cell nuclei which appeared as round hyperreflective elements with irregular hyporeflectivity inside (arrow) (b)

Table 2: Prevalence of main confocal features before and after treatment

Main features	Baseline, *n* (%)	After treatment, *n* (%)
Basal epithelial and subbasal inflammatory cells		
Dendritic cells	20/23 (87)	4/15 (23.7)
Nondendritic cells	11/23 (47.82)	4/15 (23.7)
Subbasal/anterior stromal changes		
Stippled dots in keratocyte cytoplasm	7/23 (30.43)	5/15 (33.3)
Stroma and keratocytes changes		
Activated keratocyte type 1	19/23 (82.6)	3/15 (20)
Activated keratocyte type 2	6/23 (26.1)	3/15 (20)
Endothelial changes		
KPs		
Soft large	14/23 (60.87)	0/15 (0)
Nodular	13/23 (56.53)	2/15 (13.3)
Stellate	8/23 (34.9)	0/15 (0)
Dendriform	7/23 (30.43)	0/15 (0)
Granular	6/23 (26.1)	0/15 (0)
Cruciform	7/23 (30.43)	0/15 (0)
Crumb like	1/23 (4.34)	0/15 (0)
Pseudoguttae	10/14 (71.43)	3/15 (20)
Prominent endothelial cell nuclei	9/14 (62.28)	9/15 (60)

KPs: Keratic precipitates

Early after the resolution of rejection, inflammatory cells at basal epithelial and subbasal area decreased significantly but did not disappear completely. It seems that it may take a longer period for the inflammatory cells to reach baseline density and morphology. Although the rejection episode is clinically resolved with clearance of corneal edema, KP, or other inflammatory signs, the process of rejection is still active in a subclinical state. If the anti-inflammatory treatment is discontinued at this point, exacerbation or recurrence of rejection can be anticipated.

Only keratocytes nuclei, but not their cytoplasm, can be visualized in the healthy corneal stroma.[19] They become activated in different conditions like wound healing after photorefractive keratectomy or corneal injury[20] inflammation and edema.[21] It has been shown that although these cells are metabolically activated with enlarged endoplasmic reticulum, stromal edema is an important factor contributing to the described appearance.[13] In stromal edema, increased difference in refractive index between the cells and the adjacent matrix makes cell borders and cellular processes more visible.[22]

In our study, highly AKs were more often seen in edematous corneas. It seems that regardless of the inflammatory process of rejection, corneas without significant edema will not reveal high degree AKs. However, this hypothesis requires further investigation.

We also observed stippled bright dots confined to the cytoplasm of type 1 AKs in anterior stroma in some of the patients. We postulate that these bright dots represent the active protein-synthesizing endoplasmic reticulum of a metabolically active cell and could be a more characteristic morphologic sign of AKs. Niederer *et al*. also described AKs with visible cytoplasmic processes and hyperreflective intracellular granules as nonspecific manifestation of stromal inflammation posterior to foci of DCs in Bowman's layer.[4] Type 2 AKs, the less frequently described phenotype, are cells with highly reflective nuclei with spindle-shaped morphology. They represent migratory fibroblasts which increase as a consequence of keratocyte loss and inflammation.[13] Their morphology and relation to inflammation have been more consistently explained in literature.[13] Spindle-shaped elongated AKs increase in number 2 months prior to the diagnosis of rejection and may be the first sign of subclinical rejection.[23] Similar to our findings, it has been shown that the number of AKs reaches a maximum at the time of diagnosis of the rejection but does not decrease significantly until 1 month after initiation of treatment.[23] This morphology could reflect intrastromal inflammation and does not resolve early after the resolution of graft rejection.

Aggregation of different types of KPs such as soft large (the most prevalent type), nodular, stellate, dendriform, granular, small polymorphous, and cruciform was seen at the time of rejection. Some studies tried to find an association between morphologic characteristics of KPs and the underlying disease. Cluster and nodular KPs[12] were associated with infectious uveitis. Smooth-rounded KPs were significantly more common in noninfectious uveitis.[24] The morphologic description of KPs is not consistent among all these studies. The soft large KP in this study mostly resembles the smooth-rounded KPs described by Rezaei Kanavi *et al*.[24] We observed that the dendriform and stellate KPs that were previously reported to be associated with infectious uveitis were prevalent in graft rejection, which is not an infectious process.[7,25] The correlation between the type of KPs in graft

rejection and the underlying pathology necessitating corneal grafting was not investigated in this study.

Other detectable endothelial changes were pseudoguttae,[26] polymorphism and polymegathism, and prominent endothelial cell nuclei.[27] After the resolution of rejection, KPs completely disappeared in almost all patients. The only visible endothelial change was prominent endothelial nuclei which might be a sign of stress on endothelial cells.[27]

This study had some limitations. A small sample size, unavailability of IVCM images for all the included patients having posttreatment, and short follow-up time were the main drawbacks. We could not investigate the probable association between confocal features and other variables such as causes of transplantation, treatment type, and time to resolution of rejection due to the small sample size. We only included patients whose degree of corneal edema allowed imaging of deep layers, which may be a source of bias towards selecting less severe forms of graft rejection. The IVCMs were performed early after the resolution of rejection. The time of IVCM imaging was variable among the patients, depending on the time the patient visited the doctor or time course of rejection reversal in each patient. Future studies can focus on specific time points with a longer follow-up time.

In this study, IVCM features of acute graft rejection before and after treatment of rejection were demonstrated. Activation of keratocytes, infiltration of DCs in subbasal area, and appearance of various types of KPs happen in the process of graft rejection. However, early after clinical resolution of rejection, the infiltration of activated DCs subsides and activity of keratocytes decreases but does not return to normal. KPs are the only feature that disappear completely, leaving stressed endothelial cells with prominent nuclei. It seems that at the time of clinical resolution of inflammation, the process of rejection is not completely subsided at the cellular level. IVCM can be a helpful tool in the management of corneal graft rejection.

Financial support and sponsorship
Nil.

Conflicts of interest
There are no conflicts of interest.

References

1. Jonas JB, Rank RM, Budde WM. Immunologic graft reactions after allogenic penetrating keratoplasty. Am J Ophthalmol 2002;133:437-43.
2. Panda A, Vanathi M, Kumar A, Dash Y, Priya S. Corneal graft rejection. Surv Ophthalmol 2007;52:375-96.
3. Cohen RA, Chew SJ, Gebhardt BM, Beuerman RW, Kaufman HE, Kaufman SC. Confocal microscopy of corneal graft rejection. Cornea 1995;14:467-72.
4. Niederer RL, Sherwin T, McGhee CN. *In vivo* confocal microscopy of subepithelial infiltrates in human corneal transplant rejection. Cornea 2007;26:501-4.
5. Chirapapaisan C, Abbouda A, Jamali A, M mali RT, Cavalcanti BM, Colon C, *et al. In vivo* confocal microscopy demonstrates increased immune cell densities in corneal graft rejection correlating with signs and symptoms. Am J Ophthalmol 2019;203:26-36.
6. Hau S, Clarke B, Thaung C, Larkin DFP. Longitudinal changes in corneal leucocyte density *in vivo* following transplantation. Br J Ophthalmol 2019;103:1035-41.
7. Wertheim MS, Mathers WD, Planck SJ, Martin TM, Suhler EB, Smith JR, *et al. In vivo* confocal microscopy of keratic precipitates. Arch Ophthalmol 2004;122:1773-81.
8. Hashemian MN, Latifi G, Ghaffari R, Ghassemi H, Zarei-Ghanavati M, Mohammadi SF, *et al.* Topical tacrolimus as adjuvant therapy to corticosteroids in acute endothelial graft rejection after penetrating keratoplasty: A randomized controlled trial. Cornea 2018;37:307-12.
9. Hudde T, Minassian DC, Larkin DF. Randomised controlled trial of corticosteroid regimens in endothelial corneal allograft rejection. Br J Ophthalmol 1999;83:1348-52.
10. Jabs DA, Nussenblatt RB, Rosenbaum JT; Standardization of Uveitis Nomenclature (SUN) Working Group. Standardization of uveitis nomenclature for reporting clinical data. Results of the First International Workshop. Am J Ophthalmol 2005;140:509-16.
11. Postole AS, Knoll AB, Auffarth GU, Mackensen F. *In vivo* confocal microscopy of inflammatory cells in the corneal subbasal nerve plexus in patients with different subtypes of anterior uveitis. Br J Ophthalmol 2016;100:1551-6.
12. Lim LL, Xie J, Chua CC, Wong T, Hoang LT, Becker MD, *et al. In vivo* laser confocal microscopy using the HRT-rostock cornea module: diversity and diagnostic implications in patients with uveitis. Ocul Immunol Inflamm 2018;26:900-9.
13. Hovakimyan M, Falke K, Stahnke T, Guthoff R, Witt M, Wree A, *et al.* Morphological analysis of quiescent and activated keratocytes: A review of *ex vivo* and *in vivo* findings. Curr Eye Res 2014;39:1129-44.
14. Zhivov A, Stave J, Vollmar B, Guthoff R. *In vivo* confocal microscopic evaluation of langerhans cell density and distribution in the corneal epithelium of healthy volunteers and contact lens wearers. Cornea 2007;26:47-54.
15. Hau S, Clarke B, Thaung C, Larkin DF. Longitudinal changes in corneal leucocyte density *in vivo* following transplantation. Br J Ophthalmol 2018;2019;103:1035-41.
16. Zhivov A, Stave J, Vollmar B, Guthoff R. *In vivo* confocal microscopic evaluation of Langerhans cell density and distribution in the normal human corneal epithelium. Graefes Arch Clin Exp Ophthalmol 2005;243:1056-61.
17. Mastropasqua L, Nubile M, Lanzini M, Carpineto P, Ciancaglini M, Pannellini T, *et al.* Epithelial dendritic cell distribution in normal and inflamed human cornea: *In vivo* confocal microscopy study. Am J Ophthalmol 2006;142:736-44.
18. Wang D, Song P, Wang S, Sun D, Wang Y, Zhang Y, *et al.* Laser scanning *in vivo* confocal microscopy of clear grafts after penetrating keratoplasty. Biomed Res Int 2016;2016:5159746.
19. Erie JC, Patel SV, McLaren JW, Hodge DO, Bourne WM. Keratocyte density in the human cornea after photorefractive keratectomy. Arch Ophthalmol 2003;121:770-6.
20. West-Mays JA, Dwivedi DJ. The keratocyte: Corneal stromal cell with variable repair phenotypes. Int J Biochem Cell Biol 2006;38:1625-31.
21. Alomar TS, Al-Aqaba M, Gray T, Lowe J, Dua HS. Histological and confocal microscopy changes in chronic corneal edema: Implications for endothelial transplantation. Invest Ophthalmol Vis Sci 2011;52:8193-207.
22. Masters BR, Kino GS. Confocal microscopy of the eye. In: Noninvasive Diagnostic Techniques in Ophthalmology. New York: Springer; 1990. p. 152-71.
23. Kocaba V, Colica C, Rabilloud M, Burillon C. Predicting corneal graft rejection by confocal microscopy. Cornea 2015;34 Suppl 10:S61-4.
24. Kanavi MR, Soheilian M, Naghshgar N. Confocal scan of keratic precipitates in uveitic eyes of various etiologies. Cornea 2010;29:650-4.
25. Mahendradas P, Shetty R, Narayana KM, Shetty BK. *In vivo* confocal microscopy of keratic precipitates in infectious versus noninfectious uveitis. Ophthalmology 2010;117:373-80.
26. Krachmer JH, Schnitzer JI, Fratkin J. Cornea pseudoguttata: A clinical and histopathologic description of endothelial cell edema. Arch Ophthalmol 1981;99:1377-81.
27. Patel DV, Phua YS, McGhee CN. Clinical and microstructural analysis of patients with hyper-reflective corneal endothelial nuclei imaged by *in vivo* confocal microscopy. Exp Eye Res 2006;82:682-7.